Full Text View

Volume 30, Issue 12 (December 2000)

Journal of Physical Oceanography
Article: pp. 3025–3038 | Abstract | PDF (213K)

Effects of Double Diffusion and Turbulence on Interleaving at Baroclinic Oceanic Fronts

Natalia Kuzmina and Victor Zhurbas

Shirshov Institute of Oceanology, Moscow, Russia

(Manuscript received July 7, 1998, in final form January 7, 2000)

DOI: 10.1175/1520-0485(2000)030<3025:EODDAT>2.0.CO;2

ABSTRACT

Treating the problem of interleaving in ocean fronts, a linear stability analysis is applied to a thermohaline, baroclinic front in which the vertical diffusivity for mass and momentum is determined by both the double diffusion and turbulence. If the mass and momentum diffusivity is controlled by double diffusion solely, interleaving in baroclinic fronts is possible at any value of the geostrophic Richardson number Ri. However, it is shown that turbulent mixing always works to suppress double-diffusive interleaving. Due to turbulent mixing, at some range of the input parameters there is a range of Ri where the maximum growth rate of interleaving, ω'_{max}, vanishes. Several asymptotic criteria governing the Ri dependence of ω'_{max} are found. These criteria fit well the results of numerical calculations of ω'_{max}(Ri). One of the criteria has been applied to describe intrusions observed in the Azores Front of the North Atlantic.

1. Introduction

It is known that in an inviscid adiabatic fluid the instability of a geostrophically balanced baroclinic 2D front with respect to lateral intrusive-like motion cannot occur unless the geostrophic Richardson number $\mathrm{Ri} = (f/N\gamma_\rho)^2$ is less than one (McIntyre 1970). Here, f is the Coriolis parameter, N is the Brunt–Väisälä frequency, and γ_ρ is the slope of isopycnals with respect to the horizontal. According to McIntyre (1970), this instability is referred as the symmetric classical instability. The same criterion for instability, Ri < 1, is valid for the case of viscous fluid provided that Pr = 1, where Pr is the Prandtl number, that is, the ratio of momentum to mass transfer coefficients. However, if Pr ≠ 1 the viscous/diffusive destabilization of the flow is possible (McIntyre 1970), and the criterion for monotonic instability generalizes to $\mathrm{Ri} < \mathrm{Ri}^*_M$, where $\mathrm{Ri}^*_M = (1 + \mathrm{Pr})^2/4\ \mathrm{Pr}$. Since $\mathrm{Ri}^*_M > 1$ both for Pr < 1 and Pr > 1, the viscous/diffusive destabilization of geostrophic flow at $1 < \mathrm{Ri} < \mathrm{Ri}^*_M$ is referred as the McIntyre instability.

In the case of interleaving at baroclinic fronts in the ocean, the vertical mass and momentum transfer may be governed by double diffusion and Ri-dependent turbulent mixing. Therefore, one may expect some changes in the above criteria for instability.

Since the pioneering work by Stern (1967), several models of double-diffusively driven interleaving have been developed for the purely thermohaline front with no baroclinicity (Ruddick and Turner 1979; Toole and Georgi 1981; McDougall 1985a, b; Niino 1986; Walsh and Ruddick 1995). The first model treating the effects of baroclinicity and turbulent mixing on double-diffusive interleaving in the framework of linear stability problem was suggested by Kuzmina and Rodionov (1992), hereafter referred as KR92. Further development of the KR92 model has been recently undertaken by May and Kelley (1997).

Analyzing examples of numerically computed Ri dependence of $\omega'_{\max}$ taken from KR92 convinced us that the double-diffusive destabilization of baroclinic fronts is possible even at Ri > Ri^*_M. In this paper, we will focus on determining new criteria for instability in the cases under consideration.

2. Formulation of the problem and governing equations

In the wake of KR92, let us consider an infinitely wide, baroclinic thermohaline front with constant background gradients of temperature ($\overline{T}_x$ and $\overline{T}_z$), salinity ($\overline{S}_x$ and $\overline{S}_z$), and density ($\overline{\rho}_x = -\overline{T}_x + \overline{S}_x$ and $\overline{\rho}_z = -\overline{T}_z + \overline{S}_z$) both in the cross frontal and vertical directions (the x and z axes, respectively). To simplify the notation, by T, S, and ρ we will imply the product of the thermal expansion coefficient α with temperature, the product of the salinity contraction coefficient β with salinity, and the ratio of density to the reference density ρ_0, respectively. The z axis is directed upward. The x axis is directed across the front in such a way that $\overline{S}_x \geq 0$ while $\overline{T}_x$ and $\overline{\rho}_x$ can be both positive and negative. The background stratification is assumed to be hydrostatically stable (i.e., $\overline{\rho}_z < 0$) and favorable for salt fingering ($0 < \overline{S}_z < \overline{T}_z$).

The base state is the geostrophically balanced flow

$$-f\overline{v} = -\frac{\partial \overline{p}}{\partial x} \qquad (1)$$

$$\frac{\partial \overline{p}}{\partial z} = -g\overline{\rho}, \qquad (2)$$

where v is the y-component of background velocity, $\overline{p}$ is the mean pressure divided by ρ_0, g is the gravitational acceleration, and $\overline{\rho}$ is the mean density. According to (1) and (2), the vertical shear, v_z, is related to horizontal density gradient by the thermal wind relationship,

$$\overline{v}_z = -\frac{g}{f}\overline{\rho}_x.$$

According to KR92, the linearized governing equations for two dimensional perturbations are

$$\frac{\partial u}{\partial t} - fv = -\frac{\partial p}{\partial x} + \mathrm{Pr}k\frac{\partial^2 u}{\partial z^2} + \mathrm{Pr}k^*\frac{\partial^2 u}{\partial z^2} \qquad (3)$$

$$\frac{\partial v}{\partial t} + fu + w\overline{v}_z = \mathrm{Pr}k\frac{\partial^2 v}{\partial z^2} + \mathrm{Pr}k^*\frac{\partial^2 v}{\partial z^2} \qquad (4)$$

$$\frac{\partial p}{\partial z} = -g\rho \qquad (5)$$

$$\frac{\partial u}{\partial x} + \frac{\partial w}{\partial z} = 0 \qquad (6)$$

$$\frac{\partial S}{\partial t} + u\overline{S}_x + w\overline{S}_z = k\frac{\partial^2 S}{\partial z^2} + k^*\frac{\partial^2 S}{\partial z^2} \qquad (7)$$

$$\frac{\partial \rho}{\partial t} + u\overline{\rho}_x + w\overline{\rho}_z = (1-n)k\frac{\partial^2 S}{\partial z^2} + k^*\frac{\partial^2 \rho}{\partial z^2}, \qquad (8)$$

where u, v, w, p, S, ρ are perturbations of velocity components, pressure, salinity, and density, k is the apparent diffusivity for salt due to salt fingering, k^* is the apparent diffusivity for salt, heat, and mass due to the small-scale turbulence, $n = \alpha F_T/\beta F_S$ is the nondimensional flux ratio for salt fingering ($n < 1$). Following Stern (1967), the momentum balance in the vertical direction is reduced to the hydrostatic relationship (5) implying that the slope of intrusions is small, that is, intrusive motions are quasihorizontal. The first term on the right side of (7) and (8) is the parameterization of salinity

and mass fluxes due to salt fingering suggested by Stern (1967); the second term describes the effect of small-scale turbulence. Similarly, the last two terms in the right side of (3) and (4) describe the viscosity caused by salt fingering and wave/turbulence mixing, respectively. Note that the effect of viscosity on thermohaline intrusions was first studied by Stommel and Fedorov (1967) and then incorporated into the Stern's problem by Toole and Georgi (1981). Following Kuzmina and Rodionov (1992), the effect of baroclinicity is presented by the terms $w\mathfrak{V}_z$ in (4) and $u\bar{\rho}_x$ in (8).

To perform a linear stability analysis of infinitely wide, baroclinic, thermohaline fronts, we have to seek harmonic solutions for the Eqs. (1)–(8), namely

$$\Psi = \mathrm{Re}\{\Psi' \exp(\omega t + ilx + imz)\}, \quad (9)$$

where Ψ denotes any of variables under consideration (u, $\mathfrak{V}$, w, p, S, or ρ); Ψ' is the complex amplitude for Ψ; Re is real part of $\{ \cdots \}$; ω is the growth rate (real or complex); l and m are the cross-front and vertical wavenumbers, respectively.

The problem (1)–(9) is just the same considered in KR92 and is two-dimensional. Being applied to the thermohaline front with no baroclinicity, all the above-mentioned models except (Niino 1986) treated the 3D interleaving, that is, intrusions were allowed to have a nonzero along-front tilt. When considering 3D interleaving in baroclinic fronts one has to add into the Eqs. (3)–(8) the background advection terms, that is, $\mathfrak{V}\partial u/\partial y$, etc. Since $\mathfrak{V} = \mathfrak{V}_0 + \mathfrak{V}_z z$, where $\mathfrak{V}_0$ is the mean velocity at $z = 0$, the perturbation equations for 3D problem in the baroclinic front are no longer autonomous. That is, the simple harmonic form of solution [$\sim \exp(\omega t + il_x x + il_y y + il_z z)$] is no longer valid, and, in general, we have to solve a complex, eigen function problem. For this reason, dealing with the baroclinic front we focus on a relatively simple, 2D problem.

3. Instability models

Substituting (9) into (3)–(8) gives a system of linear, homogeneous, algebraic equations. Therefore, a solution of the form (9) exists only if the determinant of this system vanishes. This yields the following quartic relationship in ω between the growth rate and wavenumbers:

$$\omega^4 + C_3\omega^3 + C_2\omega^2 + C_1\omega + C_0 = 0, \quad (10)$$

where

$$\begin{aligned}
\frac{C_0}{k^2m^4} = {} & \mathrm{Pr}(1+\zeta)N^2\left[\varepsilon_z\frac{l}{m}\left(\frac{l}{m}-\frac{\overline{S}_x}{\overline{S}_z}\right)\right. \\
& \left. + (1+\zeta)\frac{l}{m}\left(\frac{l}{m}-\frac{\overline{\rho}_x}{\overline{\rho}_z}\right)\right] \\
& + \zeta(\zeta+1) \\
& \times\left[\mathrm{Pr}^2(1+\zeta)^2k^2m^4 - N^2\frac{l}{m}\frac{\overline{\rho}_x}{\overline{\rho}_z} + f^2\right] \qquad (11) \\
\frac{C_1}{km^2} = {} & N^2\left[\varepsilon_z\frac{l}{m}\left(\frac{l}{m}-\frac{\overline{S}_x}{\overline{S}_z}\right)\right. \\
& \left. + (\mathrm{Pr}+1)(1+\zeta)\frac{l}{m}\left(\frac{l}{m}-\frac{\overline{\rho}_x}{\overline{\rho}_z}\right)\right] \\
& + \mathrm{Pr}^2k^2m^4(1+\zeta)^2\left[1+2\zeta+\frac{2\zeta}{\mathrm{Pr}}\right] \\
& - (1+2\zeta)N^2\frac{l}{m}\frac{\overline{\rho}_x}{\overline{\rho}_z} + (1+2\zeta)f^2 \qquad (12) \\
C_2 = {} & N^2\frac{l}{m}\left(\frac{l}{m}-2\frac{\overline{\rho}_x}{\overline{\rho}_z}\right)
\end{aligned}$$

$$+ \mathrm{Pr}(1+\zeta)k^2m^4\left[\mathrm{Pr}(1+\zeta)+2+4\zeta+\frac{\zeta}{\mathrm{Pr}}\right] + f^2 \quad (13)$$

$$C_3 = km^2[2\mathrm{Pr}(1+\zeta)+1+2\zeta], \quad (14)$$

where $\zeta = k^*/k$ is the ratio of turbulent to salt fingering vertical diffusivities, $\mathfrak{E}_z = (1-n)/(R_\rho - 1)$ is a nondimensional measure of contribution of the mean salinity gradient to the vertical density gradient scaled by the efficiency of density diffusion by salt fingering introduced by Toole and Georgi (1981), $R_\rho = \bar{T}_z/\bar{S}_z$ is the density ratio ($R_\rho > 1$ when the stratification is favorable for salt fingering), $N^2 = -g\bar{\rho}_z$ is the squared Brunt–Väisälä frequency.

Introducing the following nondimensional variables and parameters

$$l' = lL, \qquad m' = mH, \qquad \omega' = \omega\frac{H^2}{k},$$

$$H = \left(\frac{\mathrm{Pr}k}{f}\right)^{1/2}, \qquad \frac{H}{L} = \varepsilon_z\frac{\bar{S}_x}{\bar{S}_z}, \qquad \chi = \frac{f}{N}\frac{L}{H},$$

where L and H are typical horizontal and vertical scales of intrusion, we rewrite (10)–(14) in a nondimensional form

$$\omega'^4 + Q_3\omega'^3 + Q_2\omega'^2 + Q_1\omega' + Q_0 = 0 \quad (10')$$

$$\frac{Q_0\chi^2}{\mathrm{Pr}^2m'^4} = \mathrm{Pr}(1+\zeta)\left\{\varepsilon_z\left(\frac{l'}{m'}\right)^2 - \frac{l'}{m'} + (1+\zeta)\left[\left(\frac{l'}{m'}\right)^2 - \mathrm{sign}(\gamma_S\gamma_\rho)\chi\mathrm{Ri}^{-1/2}\frac{l'}{m'}\right]\right\} + \zeta(1+\zeta)\left[(1+\zeta)^2\chi^2m'^4 - \mathrm{sign}(\gamma_S\gamma_\rho)\chi\mathrm{Ri}^{-1/2}\frac{l'}{m'} + \chi^2\right] \quad (11')$$

$$\frac{Q_1\chi^2}{\mathrm{Pr}^2m'^2} = [\varepsilon_z + (\mathrm{Pr}+1)(1+\zeta)]\left(\frac{l'}{m'}\right)^2 - \frac{l'}{m'} - \mathrm{sign}(\gamma_S\gamma_\rho)[(\mathrm{Pr}+1)(1+\zeta)+1+2\zeta]\chi\mathrm{Ri}^{-1/2}\frac{l'}{m'} + \left[(1+\zeta)^2\left(1+2\zeta+\frac{2\zeta}{\mathrm{Pr}}\right)m'^4 + 1 + 2\zeta\right]\chi^2 \quad (12')$$

$$\frac{Q_2\chi^2}{\mathrm{Pr}^2} = \left(\frac{l'}{m'}\right)^2 - 2\,\mathrm{sign}(\gamma_S\gamma_\rho)\chi\mathrm{Ri}^{-1/2}\frac{l'}{m'} + \left\{\frac{(1-\zeta)[(1-\zeta)\mathrm{Pr}+2+4\zeta+\zeta/\mathrm{Pr}]}{\mathrm{Pr}}m'^4 + 1\right\}\chi^2 \quad (13')$$

$$Q_3 = m'^2[2\mathrm{Pr}(1+\zeta)+1+2\zeta], \quad (14')$$

(Click the equation graphic to enlarge/reduce size)

where $Q_0 = C_0H^8/k^4$, $Q_1 = C_1H^6/k^3$, $Q_2 = C_2H^4/k^2$, $Q_3 = C_3H^2/k$ are nondimensional coefficients of (10′), $\gamma_S = -\bar{S}_x/\bar{S}_z$ is the cross-front slope of isohalines.

If $Q_0 < 0$, we are assured of at least one real root for which ω is greater than zero (e.g., Stern 1967), and a growing, nonoscillating intrusion exists. Since we are going to find out new criteria for monotonic instability, we have to examine when the condition $Q_0 < 0$ being sufficient is necessary as well. In general, the number of positive real roots of a polynomial with real coefficients $Q_n, Q_{n-1}, \ldots, Q_0$ either is equal to the number N_a of sign changes in the sequence $Q_n, Q_{n-1}, \ldots, Q_0$ of coefficients, or it is less than N_a by a positive even integer (so-called Descartes rule of signs; Korn and Korn 1968). It means that at least one positive root does exist if the number of sign changes in the sequence of coefficients is an odd positive integer. Because in our quartic polynomial (10′) $Q_4 = 1$ and $Q_3 > 0$ at any $\mathrm{Pr} > 0$, the Descartes rule yields the following sufficient conditions for instability

1. $Q_0 < 0, Q_1 > 0, Q_2 > 0$;
2. $Q_0 < 0, Q_1 < 0, Q_2 > 0$;
3. $Q_0 < 0, Q_1 > 0, Q_2 < 0$;

4. $Q_0 < 0, Q_1 < 0, Q_2 < 0$.

Therefore, the above four cases can be reduced to the single sufficient condition for monotonic instability, namely, $Q_0 < 0$. Moreover, if $Q_0 < 0$, $Q_1 > 0$, $Q_2 > 0$, we are assured of one and only one positive root while if $Q_0 > 0$, $Q_1 > 0$, $Q_2 > 0$, we are assured of no one positive root. Therefore, $Q_0 < 0$ is the criterion for instability—a necessary and sufficient condition, provided that $Q_1 > 0$, $Q_2 > 0$. One more sufficient condition for instability and respective criterion will be introduced in section 3e. In the following, we will consider these conditions and criteria in more detail.

To start with, let us consider the case of no turbulent mixing. With $\zeta = 0$, (11′)–(14′) reduces to a simpler form:

$$Q_0 = \frac{\mathrm{Pr}^3 m'^4}{\chi^2}\left[\varepsilon_z\left(\frac{l'}{m'}\right)^2 - \frac{l'}{m'} + \left(\frac{l'}{m'}\right)^2 - \mathrm{sgn}(\gamma_\rho\gamma_S)\chi\mathrm{Ri}^{-1/2}\frac{l'}{m'}\right] \tag{11″}$$

$$Q_1 = \frac{\mathrm{Pr}^2 m'^2}{\chi^2}\left\{(\varepsilon_z + 1 + \mathrm{Pr})\left(\frac{l'}{m'}\right)^2 - [1 + \mathrm{sgn}(\gamma_S\gamma_\rho)(\mathrm{Pr} + 2)\chi\mathrm{Ri}^{-1/2}]\frac{l'}{m'} + (m'^4 + 1)\chi^2\right\} \tag{12″}$$

$$Q_2 = \frac{\mathrm{Pr}^2}{\chi^2}\left[\left(\frac{l'}{m'}\right)^2 - 2\,\mathrm{sgn}(\gamma_\rho\gamma_S)\chi\mathrm{Ri}^{-1/2}\frac{l'}{m'} + \left(\frac{\mathrm{Pr} + 2}{\mathrm{Pr}}m'^4 + 1\right)\chi^2\right] \tag{13″}$$

$$Q_3 = m'^2(2\mathrm{Pr} + 1). \tag{14″}$$

The right side of (11") consists of four terms. Two of them, the second and the fourth, can be negative, so two types (mechanisms) of instability do exist. The second term is responsible for thermohaline, double-diffusive instability which was discovered by Stern (1967). The fourth term is responsible for another type of instability which can exist only in baroclinic fronts. The last type of instability has been already described by Kuzmina and Rodionov (1992), and a question arises whether this instability is really a new one or is a modification of the McIntyre instability.

According to (11"), when $\chi\,\mathrm{Ri}^{-1/2} \ll 1$, $\chi\,\mathrm{Ri}^{-1/2} \gg 1$, and $\chi\,\mathrm{Ri}^{-1/2} \approx 1$ the instability is determined by thermohaline, baroclinic, and both factors, respectively. Therefore, being first introduced in KR92, the $\chi\,\mathrm{Ri}^{-1/2}$ criterion makes it possible to recognize which factors, thermohaline or baroclinic, dominates in double-diffusive interleaving in an oceanic front. Note that in accordance with (11), one can write the following expression for $\chi\,\mathrm{Ri}^{-1/2}$:

$$\chi\,\mathrm{Ri}^{-1/2} = |\gamma_\rho/\gamma_S|/\varepsilon_z.$$

Let us consider different limits (asymptotic) of (11") and (11′).

a. Double-diffusive interleaving controlled by thermohaline factors

When $\chi\,\mathrm{Ri}^{-1/2} \ll 1$, the last term in and (11") can be dropped, and the consideration reduces to a well-known case of double-diffusive interleaving in purely thermohaline fronts with no baroclinicity (Stern 1967; Toole and Georgi 1981, and their followers). Substituting $\overline{\rho}_x = 0$, $\zeta = 0$ into (11) and applying $C_0 < 0$, we can find an instability condition in terms of intrusion slopes:

$$0 < \frac{l}{m} < \left(\frac{l}{m}\right)_{\max} = \frac{R_\rho - 1}{R_\rho - n}\frac{\overline{S}_x}{\overline{S}_z} = \frac{\varepsilon_z + 1}{\varepsilon_z + 1}\frac{\overline{S}_x}{\overline{S}_z}. \quad (15)$$

Manipulating (15), one can show that if the intrusion is tilted with the maximum slope allowed for instability $(l/m)_{\max}$, the along-intrusion density ratio $\Delta T/\Delta S$ (where ΔT and ΔS are the along-intrusion gradients of temperature and salinity) will equal the flux ratio:

$$(\Delta T/\Delta S)|_{l/m=(l/m)_{\max}} = n. \quad (15')$$

b. Double-diffusive interleaving controlled by both thermohaline and baroclinic factors

If $\chi\,\mathrm{Ri}^{-1/2} \approx 1$, both factors, thermohaline and baroclinic, are important, and (11") yields the following expression for the slope of growing intrusions (May and Kelley 1997):

$$0 < \frac{l}{m} < \left(\frac{l}{m}\right)_{\max} = \frac{\varepsilon_z(\overline{S}_x/\overline{S}_z) + (\overline{\rho}_x/\overline{\rho}_z)}{\varepsilon_z + 1}. \quad (16)$$

It is clear that (15) is a partial case of (16). Moreover, manipulating (16) one can show that the along-intrusion density ratio for the growing intrusion of the maximum slope equals the flux ratio, that is, the expression (15′) is valid even in baroclinic fronts. It is worth noting that the expression (15′) differs from what was written by May and Kelley (1997) who declared that the same is valid for the fastest-growing intrusion, that is,

$$(\Delta T/\Delta S)|_{l/m=\gamma_{\max}} = n, \qquad \gamma_{\max} = \left(\frac{l}{m}\right)_{\omega=\omega_{\max}},$$

where $\omega_{\max}$ is the growth rate of fastest-growing intrusion. Since the maximum slope of growing intrusion is about twice as large as the slope of the fastest-growing intrusion,

$$\left(\frac{l}{m}\right)_{\max} \approx 2\left(\frac{l}{m}\right)_{\omega=\omega_{\max}},$$

(e.g., May and Kelley 1997) there is no reason to expect that observed values of the along-intrusion density ratio do equal the double-diffusive flux ratio. The last statement is of primary importance when dealing with observations of intrusions in the ocean.

It is interesting that double-diffusive interleaving can exist even in baroclinic fronts with no thermoclinicity, that is, when isopycnals, isohalines, and, consequently, isotherms have the same slope ($\gamma_\rho = \gamma_S = \gamma_T$, where $\gamma_T = -\overline{T}_x/\overline{T}_z$). In this case, (16) yields $(l/m)_{\max} = \overline{\rho}_x/\overline{\rho}_z$.

c. Double-diffusive interleaving controlled by baroclinic factor

If $\chi\,\mathrm{Ri}^{-1/2} = |\gamma_\rho/\gamma_S|/\varepsilon_z \gg 1$, (16) reduces to

$$0 < \frac{l}{m} < \frac{1}{\varepsilon_z + 1}\frac{\overline{\rho}_x}{\overline{\rho}_z} = \frac{R_\rho - 1}{R_\rho - n}\frac{\overline{\rho}_x}{\overline{\rho}_z} < \frac{\overline{\rho}_x}{\overline{\rho}_z}. \quad (17)$$

In this case, the slope of growing intrusions is limited by the slope of isopycnals, and can be much greater than slopes of both isohalines and isotherms, in accordance with a relationship $\gamma_\rho = (\gamma_T R_\rho - \gamma_S)/(R_\rho - 1)$. Therefore, this instability may be identified as a form of baroclinic instability. However, in contrast to the symmetric classical baroclinic instability that works only if $\mathrm{Ri} < 1$, and the McIntyre instability that cannot occur unless $1 < \mathrm{Ri} < \mathrm{Ri}^*_M$, the double-diffusive destabilization of the baroclinic front can occur with no limitation on Ri, in accordance with (11"). Therefore, at $\mathrm{Ri} > \mathrm{Ri}^*_M$ and $\chi\,\mathrm{Ri}^{-1/2} \gg 1$, the double-diffusive interleaving controlled by baroclinic factors may be considered as a new form of baroclinic instability.

The physical reason for the baroclinic instability effected by double diffusion to occur at any value of Ri lies in the fact that the case $\chi\,\mathrm{Ri}^{-1/2} \gg 1$ may be interpreted as a limiting case when $(1 - n)$ vanishes. Indeed, $n \to 1$ causes $\chi\,\mathrm{Ri}^{-1/2} \gg 1$ and $(l/m)_{\max} \to \overline{\rho}_x/\overline{\rho}_z$. Moreover, in accordance with (8), if $(1 - n)$ and k^* vanish, the vertical diffusion of mass vanishes too, while the diffusion of momentum still exists [see Eqs. (3) and (4)]. That is, the ratio of momentum to mass diffusivities approaches infinity, and applying the McIntyre (1970) theory we conclude that the viscous/diffusive destabilization of the flow can occur at any (large) value of Ri because $\mathrm{Ri}^*_M = (1 + \mathrm{Pr})^2/4\ \mathrm{Pr} \to \infty$.

d. Interleaving in the haline front

By haline front, we mean a thermohaline front in which the horizontal gradient of density is determined mainly by salinity rather than temperature, that is, $|R_{\rho x}| < 1$, where $R_{\rho x} = \overline{T}_x/\overline{S}_x$ is the cross-front density ratio. The relationship between isopycnal and isohaline slopes can be written as

$$\gamma_\rho = \gamma_S \frac{R_{\rho x} - 1}{R_\rho - 1}. \qquad (18)$$

The relationship (18) implies that in the haline front with the stratification favorable for salt fingering (i.e., $R_\rho > 1$) the isopycnal slope opposes the isohaline slope:sign($\gamma_\rho\ \gamma_S$) = − 1. Therefore, the second and fourth terms of (11") responsible for thermohaline and baroclinic factors of instability, respectively, are opposite in sign. In this case, thermohaline and baroclinic wedges of instability do not overlap (May and Kelley 1997). It can be shown from (16) that if $(1 - n)|\overline{S}_x/\overline{\rho}_x| > 1$, the maximum interleaving slope lies between zero and the isohaline slope, that is, the growing intrusions fall into the thermohaline wedge of instability. If $(1 - n)|\overline{S}_x/\overline{\rho}_x| < 1$, the maximum interleaving slope lies between zero and the isopycnal slope, that is, growing intrusions fall into the baroclinic wedge of instability.

Note, that if $(1 - n)|\overline{S}_x/\overline{\rho}_x| = 1$ and sign($\gamma_\rho\ \gamma_S$) = −1, thermohaline and baroclinic factors will cancel each other; the term independent of ω is not allowed to be negative, and double-diffusive interleaving controlled by both thermohaline and baroclinic factors does not exist. Therefore, the growth rates of fastest-growing intrusions in the haline front are expected to be less than those in a thermal front provided that other parameters of these fronts are the same. Moreover, assuming that larger growth rates yield larger steady state amplitudes of intrusions we may expect the intensity of intrusions to be generally higher in thermal fronts rather then haline fronts in the ocean.

It is worth noting that, in accordance with (18), sign($\gamma_\rho\ \gamma_S$) = −1 is valid also for a thermal front provided that $R_{\rho x} < -1$, that is, when mean horizontal gradients of temperature and salinity are of opposite sign. However, fronts with $R_{\rho x} < -1$ being possible are not typical for the open ocean (Fedorov 1986).

e. Instability at low Richardson numbers

In addition to $Q_0 < 0$, there is one more sufficient condition for instability, namely, $Q_2 < 0$, which is valid for our particular polynomial (10)–(10′). To prove it, let us present (10′) in a form

$$\Pi(m', \omega') = \omega'^4 + \omega'^3 m'^2 q_3 + \omega'^2[q_2 + O(m'^4)] + \omega' m'^2[q_1 + O(m'^4)] + m'^4[q_0 + O(m'^4)], \qquad (10'')$$

where q_i, i = 0, 1, 2, 3, are some functions of l'/m' and the governing parameters Pr, χ, ζ, etc., $O(\eta)$ is a function of the order of η when η vanishes, that is, $\lim_{\eta \to 0} [O(\eta)/\eta] = \text{const} \neq 0$. It is important to note that sign(q_i) = sign(Q_i). To prove our "theorem" it is enough to find some pairs (m'_0, ω'_0) and (m'_1, ω'_1), $\omega'_0, \omega'_1 > 0$, for which $\Pi(m'_0, \omega'_0) < 0$ and $\Pi(m'_1, \omega'_1) > 0$ provided that $q_2 < 0$. If we consider a partial case $m' = \omega'$, $\omega' \ll 1$ (10") reduces to

$$\Pi(m' = \omega', \omega') = \omega'^4 + \omega'^5 q_3 + \omega'^2 q_2 + \omega'^3 q_1 + \omega'^4 q_0 + O(\omega'^6). \qquad (10''')$$

It is clear from (10") and (10‴) that

$$\lim_{\omega' \to +\infty} \Pi(m' = \text{const}, \omega') = +\infty;$$

$$\lim_{\omega' \to +0} [\Pi(m' = \omega', \omega')/\omega'^2] = q_2.$$

The latter limits offer a straightforward way to find the pairs (m'_0, ω'_0) and (m'_1, ω'_1) we need.

In accordance with the above proof and the Descartes' rule, if $Q_2 < 0$, $Q_1 > 0$, $Q_0 > 0$, we are assured of two and only two positive roots in (10′), while if $Q_2 > 0$, $Q_1 > 0$, $Q_0 > 0$, we are assured of no one positive root. Therefore, $Q_2 < 0$ is the criterion for instability (a necessary and sufficient condition) provided that $Q_1 > 0$, $Q_0 > 0$.

Rewriting (13′) in a form

$$\frac{Q_2}{\mathrm{Pr}^2} = \frac{1}{\chi^2}\left(\frac{l'}{m'} - \frac{\mathrm{sgn}(\gamma_S\gamma_\rho)\chi}{\mathrm{Ri}^{1/2}}\right)^2 - \frac{1}{\mathrm{Ri}} + \frac{(1-\zeta)[(1-\zeta)\mathrm{Pr} + 2 + 4\zeta + \zeta/\mathrm{Pr}]}{\mathrm{Pr}} m'^4 + 1, \qquad (13''')$$

we find that $Q_2 < 0$ can be satisfied only if

$$\mathrm{Ri} < 1.$$

Therefore, growing modes which result from these two roots may be attributed to the symmetric classical baroclinic instability. In addition, according to (13[fy4,1]-), if $Q_2 < 0$, the following expression is valid:

$$(\xi - 1)^2 + \mathrm{Ri} - 1 < 0, \qquad (19)$$

where $\xi = (l/m)/(\bar{\rho}_x/\bar{\rho}_z)$ is the ratio of intrusion to isopycnal slopes. Equation 19 implies that the maximum slope of growing intrusions is twice as large as the isopycnal slope (because $\xi \to 2$ when $\mathrm{Ri} \to 0$). This is an important difference between the symmetric classical baroclinic instability and baroclinicity controlled double-diffusive interleaving when the slope of growing intrusions is restricted by the isopycnal slope [cf. (17)].

Since $Q_1 > 0$ is necessary for the sufficient conditions $Q_2 < 0$ and $Q_0 < 0$ to be the criteria for instability, let us consider asymptotics of (12′) at small and large ζ:

$$\frac{Q_1\chi^2}{\mathrm{Pr}^2 m'^2} = (\varepsilon_z + 1 + \mathrm{Pr})\left[\frac{l'}{m'} - \frac{1 + \mathrm{sgn}(\gamma_S\gamma_\rho)(\mathrm{Pr}+2)\chi}{2(\varepsilon_z + 1 + \mathrm{Pr})\mathrm{Ri}^{1/2}}\right]^2 - \frac{[1 + \mathrm{sgn}(\gamma_S\gamma_\rho)(\mathrm{Pr}+2)\chi\mathrm{Ri}^{-1/2}]^2}{4(\varepsilon_z + 1 + \mathrm{Pr})} + (1 + m'^4)\chi^2, \qquad \zeta \ll 1 \qquad (12'.1)$$

$$\frac{Q_1\chi^2}{\mathrm{Pr}^2 m'^2} = \zeta(\mathrm{Pr}+1)\left[\frac{l'}{m'} - \mathrm{sgn}(\gamma_S\gamma_\rho)\frac{(\mathrm{Pr}+3)\chi}{2(\mathrm{Pr}+1)\mathrm{Ri}^{1/2}}\right]^2 + 2\zeta^3\frac{\mathrm{Pr}+1}{\mathrm{Pr}}\chi^2 m'^4 + 2\zeta\chi^2\left[1 - \frac{(\mathrm{Pr}+3)^2}{8(\mathrm{Pr}+1)\mathrm{Ri}}\right], \qquad \zeta \gg 1. \qquad (12'.2)$$

In accordance with (12′.1) and (12′.2), the following conditions are sufficient for Q_1 to be positive:

$$\delta(\mathrm{Pr} + 1)$$

If $\zeta = 0$ (the case of no turbulence), the sufficient condition for instability Ri < 1 (i.e., $Q_2 < 0$) is not a criterion for instability, because, in accordance with (11''), Q_0 is allowed to be negative at any Ri < 1, except a case $\mathrm{sign}(\gamma_S\,\gamma_\rho) = -1$, $\chi\,\mathrm{Ri}^{-1/2} = 1$ when $Q_0 = 0$. All the same, if $\zeta \gg 1$ and Pr ≠ 1, the condition Ri < 1 is not the criteria for instability in view of (20.3) [see also section 3f(3)]. If $\zeta \gg 1$ and Pr = 1, the condition Ri < 1 is the criteria for instability, because in this very special case all the coefficients Q_0, Q_1, Q_2 are negative (for some values of wavenumbers) at Ri < 1 and positive at Ri > 1 for any wavenumbers [concerning Q_0, see section 3f(3)]. Finally, if $\zeta \ll 1$ (the case of weak turbulence), in accordance with (20.1), (20.2), and considerations in sections 3f(1) and (2), it is possible that Ri < 1 is the criteria for instability at some values of governing parameters Pr, χ, ζ, ε_z. The last case is just presented in Figs. 4 and 5 (for details see the description of these figures in section 5).

f. Effect of turbulent mixing on the instability

In accordance with (10′)–(14′), for given input parameters Pr, χ, ε_z, ζ, and Ri the growth rate ω' is a function of the cross-front slope ($-l'/m'$) and vertical wavenumber (m'). Maximizing ω' on ($-l'/m'$, m')-plane numerically, Kuzmina and Rodionov (1992) showed that the turbulent mixing works to suppress the double-diffusive interleaving, that is, to decrease the maximum growth rate $\omega'_{\max}$. In some cases, $\omega'_{\max}$ was found to vanish due to the turbulence. Here, we will examine this issue analytically.

In general, ζ, the ratio of turbulent to double-diffusive salt diffusivities, may be assumed to be a monotonically decreasing function of the Richardson number based on a superposition of internal-wave shear and geostrophic current shear. Physical reasons for the Ri dependence of ζ are (i) increasing probability for generation of turbulence by shear instability at low Ri and (ii) the decrease of salt finger fluxes due to vertical shear tilting over the fingers (Kunze 1994). In most oceanic situations near-inertial-internal-wave shear is larger than that of geostrophic current, so that ζ will be mainly a function of the internal-wave Richardson number which, in its turn, is governed by the Brunt–Väisälä frequency N. However, in this study we focus on the baroclinicity dependence of maximum growth rate, that is, the geostrophic Richardson number dependence of $\omega'_{\max}$ provided that N = constant. For this reason, we will assume that ζ is a decreasing function of the geostrophic Richardson number instead of the real internal-wave-influenced Richardson number. We will use for this ζ(Ri) a simple power formula

$$\zeta = A\,\mathrm{Ri}^{-\sigma}, \quad (21)$$

where $A > 0$ and $\sigma \geq 0$ are some constants. Let us consider different limits of (11′) with (21):

1) $X\,\mathrm{RI}^{-1/2} \ll 1$, $\zeta \ll 1$

In this limit, (11′) reduces to

$$\frac{Q_0\chi^2}{\mathrm{Pr}^2 m'^4} = \mathrm{Pr}(\varepsilon_z + 1)\left[\frac{l'}{m'} - \frac{1}{2(\varepsilon_z + 1)}\right]^2 - \frac{\mathrm{Pr}}{4(\varepsilon_z + 1)} + \frac{A\chi^2}{\mathrm{Ri}^\sigma}(1 + m'^4). \quad (22)$$

The first and second items in the right part of (22) describe the double-diffusive instability controlled by thermohaline factors, do not depend on Ri, and their sum is negative in the case of instability. The last item in the right side of (22) describes the effect of turbulent mixing, is positive and decreases with Ri. Therefore, due to the effect of turbulent mixing, the maximum growth rate of double-diffusive intrusions controlled by thermohaline factors is expected to fall with the decrease of Ri, in accordance with the numerical calculations by KR92.

Applying $Q_0 < 0$ to (22), we find the following sufficient conditions for instability:

$$(\sigma = 0,\ \zeta \ll 1,\ \chi \mathrm{Ri}^{-1/2} \ll 1). \quad (23.2)$$

The conditions (23) do not allow this type of instability to exist at low Ri when $\sigma > 0$ and high A when $\sigma = 0$, that is, when the turbulence is high enough to suppress the double-diffusive interleaving controlled by thermohaline factors. Sufficient condition (23.1) becomes the criterion for instability provided that $\mathrm{Ri}^*_1 > 1$ and (20.1)–(20.2) is satisfied at $\mathrm{Ri} = \mathrm{Ri}^*_1$:

2) $X\,\mathrm{RI}^{-1/2} \gg 1, \zeta \ll 1$

In this case, (11′) reduces to

$$\frac{Q_0}{\mathrm{Pr}^2 m'^4} = \frac{\mathrm{Pr}(\varepsilon_z + 1)}{\chi^2}\mathrm{Pr}(\varepsilon_z + 1)\left[\frac{l'}{m'} - \frac{\mathrm{sgn}(\gamma_S \gamma_\rho)\chi}{2(\varepsilon_z + 1)\mathrm{Ri}^{0.5}}\right]^2 - \frac{\mathrm{Pr}}{4(\varepsilon_z + 1)\mathrm{Ri}} + \frac{A(1 + m'^4)}{\mathrm{Ri}^\sigma}. \quad (24)$$

Depending of the value of σ, (24) yields the following sufficient conditions for instability:

$$\mathrm{Ri} < \mathrm{Ri}^*_2 = \left[\frac{\mathrm{Pr}}{4A(\varepsilon_z + 1)}\right]^{1/(1-\sigma)},$$
$$(0 \le \sigma < 1,\ \zeta \ll 1,\ \chi \mathrm{Ri}^{-1/2} \gg 1) \quad (25.1)$$

$$A < A_2 = \frac{\mathrm{Pr}}{4(\varepsilon_z + 1)},$$
$$(\sigma = 1,\ \zeta \ll 1,\ \chi \mathrm{Ri}^{-1/2} \gg 1) \quad (25.2)$$

$$\mathrm{Ri} > \mathrm{Ri}^*_3 = \left[\frac{4A(\varepsilon_z + 1)}{\mathrm{Pr}}\right]^{1/(\sigma-1)},$$
$$(\sigma > 1,\ \zeta \ll 1,\ \chi \mathrm{Ri}^{-1/2} \gg 1). \quad (25.3)$$

Sufficient conditions (25.1) and (25.3) become the criteria for instability provided that $\mathrm{Ri}^*_2 > 1$ and $\mathrm{Ri}^*_3 > 1$, and (20.1)–(20.2) are satisfied at $\mathrm{Ri} = \mathrm{Ri}^*_2$ and $\mathrm{Ri} = \mathrm{Ri}^*_3$, respectively.

If $0 \leqslant \sigma < 1$, the turbulent mixing decreases with Ri slowly, and there is a top Ri limit for the double-diffusive interleaving controlled by baroclinic factors to exist [formula (25.1)]. If $\sigma = 1$ the instability can exist with any value of Ri, provided that A is not too large. Finally, if $\sigma > 1$, the turbulent mixing decreases with Ri rapidly establishing a bottom Ri limit for the instability.

The above results [sections 3f(1) and 3f(2)] seem to be new findings and are worth to be discussed. First, we found that turbulent mixing is able to destroy the double-diffusive interleaving controlled by baroclinic factors, and this is an obvious difference between this instability and the McIntyre instability. Second, there is a simple physical explanation for the destructive effect of turbulence on the double-diffusive interleaving. Namely, following Zhurbas et al. (1988), we may suggest that the value of salt fingering flux ratio, n, has to be increased due to the turbulent mixing. If the intensity of turbulent mixing is sufficiently high, the flux ratio can become greater than unity. That is, the buoyancy flux changes sign, and the energy source to support interleaving vanishes.

3) $\zeta \gg 1$

Treating the case when the turbulent diffusivity is much greater than the salt finger diffusivity, we consider a limit $\zeta \to \infty$, $m'^2\zeta$ = const or, in dimensional variables, $k \to 0$, k^* = const > 0. In this limit, (11′) yields

$$+ \zeta^4 m'^8 + \zeta^2 m'^4 \left[1 - \frac{(\mathrm{Pr} + 1)^2}{4\mathrm{PrRi}}\right]. \qquad (26)$$

Substituting (26) into $Q_0 < 0$, we get

$$\mathrm{Ri} < \mathrm{Ri}^*_M = \frac{(\mathrm{Pr} + 1)^2}{4\mathrm{Pr}}. \qquad (27)$$

Note that (27) coincides well-known McIntyre criterion, in accordance with the physical reason. However, we may not consider the sufficient condition (27) as the criterion for instability unless we are assured of two items: 1) our Ri^*_M is not less than one, and 2) (20.3) is satisfied at $\mathrm{Ri} = \mathrm{Ri}^*_M$. Manipulating these items it can be easily shown that (27) is the true criterion for instability at any $\mathrm{Pr} > 0$.

4. Numerical examples

To illustrate the above theory, using (10′)–(14′), and (21) we calculate numerically the maximum growth rate of intrusions, $\omega'_{\max}$, versus Ri for different sets of input parameters Pr, χ, $\mathfrak{E}_z$, A, σ. Following KR92, we will use the geostrophic Froude number $\delta \equiv \mathrm{Ri}^{-1/2}$ instead of Ri. Being proportional to the isopycnal slope γ_ρ, this δ is referred as the baroclinicity parameter (Zhurbas et al. 1988). Calculating δ-dependencies of $\omega'_{\max}$ has been done only for $\delta \leqslant 1$ (or $\mathrm{Ri} \geq 1$) to avoid treating the case of symmetric classical instability which dominates at $\mathrm{Ri} < 1$. The problem has too many nondimensional parameters and instability criteria, and we are not able to demonstrate all the possibilities in the framework of a single paper. For this reason we restrict our consideration to the case $\mathfrak{E}_z = 0.5$, $\chi \geq 1$, $\mathrm{Pr} \geq 1$.

Figure 1 is $\omega'_{\max}$ versus δ for the following input parameters: $\mathrm{Pr} = 1$, $\chi = 10$, $A = 0$, $\mathfrak{E}_z = 0.5$. Two curves in Fig. 1 have the only difference in parameters, namely $\mathrm{sign}(\gamma_\rho \gamma_S) = 1$ (the top curve) and $\mathrm{sign}(\gamma_\rho \gamma_S) = -1$ (the bottom curve). If isohaline and isopycnal slopes are of the same sign and the turbulence is not considered, $\omega'_{\max}$ approaches some positive constant when $\delta \to 0$ (double-diffusive interleaving controlled by thermohaline factors) and increases monotonically with δ due to the baroclinicity. If the isohaline slope opposes the isopycnal slope, $\omega'_{\max}$ approaches the same value at $\delta \to 0$, decreases with δ as long as it vanishes at $\chi\delta = 1$ [second and fourth terms of (11") cancel out], and then increases with δ at $\chi\delta > 1$. This case has been considered in detail by May and Kelley (1997).

Figure 2 demonstrates the effect of turbulence on double-diffusive interleaving provided that the turbulent diffusivity k^* does not depend on Ri. Here, δ-dependence of $\omega'_{\max}$ is shown both for the cases of turbulence ($A = 0.1$, $\sigma = 0$, solid curves) and no turbulence ($A = 0$, dashed curves). Comparing respective solid and dashed curves, we conclude that turbulent mixing reduces $\omega'_{\max}$ in the whole range of δ, that is, the turbulence suppresses for double-diffusive interleaving controlled by both thermohaline and baroclinic factors, as follows from (22) and (24). To explain $\omega'_{\max}(\delta)$ curves in detail we can use the sufficient condition (23.2) and (25.1)/(20.1) criterion.

For the thin solid curve, $A = 0.1 < A_1 = 0.167$ [see (23.2)], and interleaving controlled by thermohaline factors is allowed at $\chi\delta < 1$, and, therefore, at the whole range of $\delta < 1$ (because $\chi = 1$). However, for a bold solid curve in Fig. 2, $A = 0.1 > A_1 = 1.67 \times 10^{-3}$, and interleaving controlled by thermohaline factors (at $\chi\delta < 1$, or $\delta < 0.1$) does not exist. Moreover, in the last case $\chi\,\mathrm{Ri}^{*-1/2}_2 = 7.7 \gg 1$, and in accordance with (25.1) the baroclinicity controlled, double-diffusive interleaving is allowed only at $\delta > \delta_2 \equiv \mathrm{Ri}^{*-1/2}_2 = 0.77$. The latter is the criterion for instability because (20.1) is satisfied at $\mathrm{Ri} = \mathrm{Ri}^*_2$. That is why the bold solid curve in Fig. 2 vanishes at $\delta \approx 0.59$ which is not far from $\delta_2 = 0.77$ [the criterion (25.1)/(20.1) is an asymptotic one!] and does not exist at lower δ.

Figure 3 shows the effect of turbulence on double-diffusive interleaving provided that the turbulent diffusivity k^* is weakly dependent on Ri, namely when $\sigma = 0.5$ and $A = 0.25$ are applied to (21). In this case, $\omega'_{\max}(\delta)$ curves are governed by (23.1)/(20.1), and (25.1)/(20.1) criteria. The (23.1)/(20.1) criterion predicts interleaving at $\delta < \delta_1 \equiv \mathrm{Ri}^{*-1/2}_1$ provided that $\chi\delta_1 \ll 1$ and (20.1) is satisfied at $\mathrm{Ri} = \mathrm{Ri}^*_1$, while (25.1)/(20.1) does the same at $\delta > \delta_2$ provided that $\chi\delta_2 \gg 1$ and (20.1) is satisfied at $\mathrm{Ri} = \mathrm{Ri}^*_2$. Therefore, if $\delta_1 \ll \delta_2$ one may expect that there is no interleaving in a range of $\delta_1 < \delta < \delta_2$. For a bold solid curve in Fig. 3, $\delta_1 = 6.7 \times 10^{-4}$, $\chi\delta_1 = 6.7 \times 10^{-2}$, $\delta_2 = 0.15$, $\chi\delta_2 = 15$, and (20.1) is satisfied at $\mathrm{Ri} = \mathrm{Ri}^*_1$ and $\mathrm{Ri} = \mathrm{Ri}^*_2$; the numerical calculations show that there is no positive $\omega'_{\max}$ at $7.0 \times 10^{-4} < \delta < 0.12$, which is in good correspondence with the theoretically predicted range of no interleaving. For the bold dashed curve in Fig. 3 $\delta_1 =$

7.4×10^{-3}, $\chi\delta_1 = 0.22$, $\delta_2 = 0.15$, $\chi\delta_2 = 4.5$, and (20.1) is satisfied at $Ri = Ri^*_1$ and $Ri = Ri^*_2$; the numerically calculated range of no interleaving ($0.016 < \delta < 0.065$) becomes narrower than the theoretically predicted one ($7.4 \times 10^{-3} < \delta < 0.15$).

For the rest of curves in Fig. 3 (solid, dashed and dotted), $\delta_1/\chi\delta_1$ are 1.67×10^{-2}/0.33, 6.7×10^{-2}/0.67, 0.74/2.2, respectively. Therefore, δ_1 is no longer much less than $\delta_2 = 0.15$ (for the dotted curve, δ_1 is even greater than δ_2), and ω'_{max} becomes positive for the whole range of δ.

Figure 4 shows the effect of turbulence on double-diffusive interleaving for a stronger Ri dependence of turbulent diffusivity than in Fig. 3, namely for $\sigma = 1$. In this case, $\omega'_{max}(\delta)$ curves are governed by the (23.1)/(20.1) criterion and the sufficient condition (25.2). For a bold curve, $\delta_1 = 0.041$, $\chi\delta_1 = 0.41$, $A_2 = 0.167$, and (20.1) is satisfied at $Ri = Ri^*_1$. That is, the interleaving controlled by thermohaline factors is possible approximately at $\delta < \delta_1 = 0.041$ (actually the bold curve vanishes at $\delta = 0.067$), while baroclinicity controlled interleaving disappears because $A = 1$ is much greater than $A_2 = 0.167$. There is no interleaving when δ is approaching unity from below and (20.1) is satisfied at $Ri = 1$, that is, this is just the case discussed in section 3e when the criterion for classical instability $Ri < 1$ ($Q_2 < 0$, $Q_1 > 0$, $Q_0 > 0$) does work.

The thin solid curve in Fig. 4 is $\omega'_{max}(\delta)$ for the same input parameters as those of the bold line but A is a factor 10 smaller. In this case, $\delta_1 = 0.13$, $\chi\delta_1 = 1.3$ (i.e., the (23.1)/(20.1) criterion does not work), $A = 0.1 < A_2 = 0.167$ [the sufficient condition (25.2) is satisfied], and, therefore, $\omega'_{max}(\delta)$ is positive in the whole range of δ.

The dashed line in Fig. 4 is $\omega'_{max}(\delta)$ for the same input parameters as those of the bold curve but Pr is twice greater. In this case, $\delta_1 = 0.058$, $\chi\delta_1 = 0.58$, and (20.1) is satisfied at $Ri = Ri^*_1$. Therefore, in accordance with (23.1)/(20.1), $\delta < \delta_1$, or $Ri > Ri^*_1$ is the criterion for instability (actually, ω'_{max} vanishes at $\delta = 0.137$). Then, $A = 1 > A_2 = 0.33$, that is, baroclinicity controlled interleaving does not exist. However, ω'_{max} regains the positive value at $\delta \geq 0.79$. Since $Q_0 > 0$ and $Q_2 > 0$ at $0.79 \leqslant \delta < 1$ (or $1 < Ri \leqslant 1.60$), in order to explain the existence of instability in this range we have to suggest that $Q_1 < 0$. Indeed, in accordance with (20.1) $Q_1 < 0$ at $\delta > 0.91$ or $Ri < 1.21$. Some discrepancy between the numerically computed and predicted by (20.1) ranges of instability is due to asymptotic nature of (20.1): it implies that $\zeta \ll 1$ while $A = 1$ in the case under consideration [see (21)].

Figure 5 shows the effect of turbulence on double-diffusive interleaving for a strong Ri dependence of turbulent diffusivity, namely for $\sigma = 2$. In this case, $\omega'_{max}(\delta)$ curves are governed by (23.1)/(20.1), and (25.3)/(20.1) criteria. For bold solid, bold dashed, solid, and dashed curves in Fig. 5, $\chi\delta_1$ is 6.4, 2.0, 1.1, and 0.64, respectively, that is, the condition $\chi\delta_1 \ll 1$ is not satisfied, and (23.1)/(20.1) criterion does not work. The only criterion which can explain the $\omega'_{max}(\delta)$ curves in Fig. 5 is the (25.3)/(20.1) criterion. In accordance with (25.3), interleaving is possible at $\delta < \delta_3 \equiv Ri^{*-1/2}_3$ provided that $\chi\delta_3 \gg 1$. In the case of Fig. 5, $\delta_3 = 0.41$, and $\chi\delta_3 = 41$, 4.1, 1.2, 0.41 for the bold solid, bold dashed, solid, and dashed curves, respectively. That is, for the bold solid and bold dashed curves, (25.3)/(20.1) predicts ω'_{max} to be positive at $\delta < \delta_3$ while vanishing with $\delta \to \delta_3$. Actually ω'_{max} vanishes at $\delta = 0.44$ and $\delta = 0.53$ for the bold solid and bold dashed curves, respectively, which is in a good agreement with the above asymptotic theory. Note that in these two cases (20.1) is satisfied at any $\delta \leqslant 1$, so that $Ri < 1$ ($Q_2 < 0$) is one more criterion for instability.

5. Comparison with ocean data

Using closely spaced CTD data taken from ocean fronts, one can introduce a measure of intrusion intensity, σ_T, and calculate an empirical dependence of this σ_T upon δ at constant values of the input parameters $\mathfrak{E}_z$ and χ. Assuming that larger growth rates yield larger steady state amplitudes of intrusions we may expect a correspondence between empirical dependencies $\sigma_T(\delta)$ and respective theoretical dependencies $\omega'_{max}(\delta)$. Therefore, it would be reasonable to compare empirical dependencies of $\sigma_T(\delta)$ and theoretical dependencies of $\omega'_{max}(\delta)$ provided that they have the same values of $\mathfrak{E}_z$ and χ. Despite of our inability to estimate the rest of the input parameters (Pr, A, σ) directly from CTD data, such a comparison seems useful. This approach has been applied by Kuzmina (1998), and here we consider an example of the kind.

In this example, we use the data of closely spaced CTD survey of a fragment of the Azores Front (Zhurbas et al. 1993; Kuzmina 1997). To extract the mean and finestructure fluctuations from vertical profiles of temperature and salinity, a running cosine filter with a 20-m half-window was used. The intrusion intensity was estimated as the root mean square amplitude of temperature fluctuations, σ_T, for 100-m layers. Subsequent layers had a depth overlap of 80 m. Values N and R_ρ were estimated as the mean values over a layer under consideration. To estimate locally averaged slopes γ_ρ and γ_S (or

horizontal gradients ρ_x and S_x), the central differences of respective mean values on the base of two stations closest to the present one were computed for each layer of every station. We only left for consideration empirical points with nearly constant values of $N = (4 \pm 0.5) \times 10^{-3}$.

Since the empirical estimates of ε_z are in a narrow range from 0.4 to 0.5 (provided that $n = 0.56$; Turner 1973) while χ and δ do vary in a much wider range, at least from 1 to 300 and from 0.003 to 1, respectively, we will consider a dependence of σ_T on χ and δ, suggesting that all the data may be characterized by some constant values of ε_z and Pr. It is worth noting that in our case all variations of $\delta \equiv |\gamma_\rho| N/f$ and $\chi \equiv f/N\varepsilon_z|\gamma_S|$ are controlled by slopes γ_ρ and γ_S only.

In Fig. 6, the empirical dependencies σ_T versus δ are shown for some four χ intervals: (a) $1 \leqslant \chi < 2$, (b) $5 \leqslant \chi < 10$, (c) $15 \leqslant \chi < 20$, and (d) $25 \leqslant \chi < 30$, provided that $\chi\delta < 2$ (the last inequality is to select the thermoclinicity controlled part of the dependencies only). One can see some resemblance between empirical dependencies $\sigma_T(\delta)$ in Fig. 6 and the sharply descending branches of theoretical curves $\omega'_{\max}(\delta)$ (e.g., the bold curves in Figs. 3 and 4). Moreover, a remarkable feature of these empirical $\sigma_T(\delta)$ is that a value of δ at which σ_T vanishes, decreases with the increase of χ. Note that such a behavior of empirical $\sigma_T(\delta)$ is in accordance with (23.1)/(20.1) criterion.

Figure 7 is a map of $\lg\sigma_T$ versus $\lg\chi$ and $\lg\delta$ drawn using our data. In this map, the lowest values of σ_T appear to be aligned to some line close to $\chi\delta = 1$, while at $\chi\delta \ll 1$ and $\chi\delta \gg 1$ the intrusion intensity is higher. We believe that such a behavior of $\sigma_T(\chi, \delta)$ is in accordance with the above theory of thermoclinicity and baroclinicity controlled interleaving at $\chi\delta \ll 1$ and $\chi\delta \gg 1$, respectively, implying that relatively low values of σ_T at $\chi\delta \approx 1$ are due to the suppression of interleaving by turbulence. In principle, similar behavior of $\sigma_T(\chi, \delta)$ (i.e., minimum of σ_T at $\chi\delta = 1$) may be expected in the haline front of no turbulence (see section 3d and Fig. 1). However, this is not the case because the Azores Front is a typical temperature front in which $\text{sign}(\gamma_\rho\gamma_S) = 1$.

A trough of low σ_T at $\chi\delta \approx 1$ in Fig. 7 resembles qualitatively theoretical curves $\omega'_{\max}(\delta)$ in Fig. 3. However, in contrast to theoretical curves, the observations do not display clearly an area of no interleaving because (a) there is a noise in σ_T estimates, and (b) the real value of Prandtl number is not expected to be constant so that no threshold is evident (cf. Fig. 4).

To estimate quantitatively the slope Φ of a region of low σ_T, we pick up pairs (χ, δ) for which $\lg\sigma_T < -1.8$, and calculate a slope of the major principal axis of respective cluster of points $(\lg\chi, \lg\delta)$. In Fig. 8, these points are surrounded by circles. We get $\Phi = -1.05$, and the difference of this value from -1 is not statistically significant.

It may be seen from Figs. 7 and 8 that the region of low σ_T displays a tendency to widen with χ so that the bottom boundary of this region, adjacent to $\chi\delta \ll 1$, has a slope $\Phi_1 < \Phi$ (i.e., $|\Phi_1| > |\Phi|$). To estimate Φ_1, we pick up pairs (χ, δ) for which $\lg\sigma_T < -1.8$ and $\chi\delta < 2$, and apply an approach we used to estimate Φ. We got $\Phi_1 = -1.10$, but the difference of this value from -1 was not statistically significant either.

It seems promising to identify the bottom boundary of the trough of low σ_T with a line where interleaving vanishes in accordance with (23.1),

$$\delta = \delta_1 \equiv \left[\frac{\text{Pr}}{4A(\varepsilon_z + 1)}\right]^{1/2\sigma} \chi^{-(1/\sigma)}, \qquad \sigma > 0, \quad (23.1')$$

and estimate σ, the power of Ri dependence of the turbulent mixing coefficient (21), at $\sigma = -1/\Phi_1 \approx 0.90$. Recall that, strictly speaking, (23.1) is valid when $\chi\,\text{Ri}^{-1/2} \ll 1$ and $\zeta \ll 1$, while the bottom boundary of low σ_T trough lies at $\chi\,\text{Ri}^{-1/2} < 1$ (see Fig. 7), and we may expect that $\zeta < 1$ because the Azores front is characterized by a rather low mean value of density ratio $R_\rho = 1.9$–2.0, implying relatively high level of salt finger activity. Nevertheless, we use (23.1) since a simple analytical criterion suitable to explain the observations cannot be derived on the basis of assumptions $\chi\,\text{Ri}^{-1/2} = O(1)$ and $\zeta = O(1)$. We do not use (25.1)–(25.3) conditions to compare with Fig. 7 because in contrast to (23.1) they do not yield an explicit relationship between measurable parameters χ and δ.

Unfortunately, estimates of the slopes, Φ_1 and Φ, and, therefore, σ may be biased, as it was pointed out by anonymous reviewer. Let us consider this issue in more detail.

In general, it is possible that estimates of the slopes Φ_1 and Φ are biased due to inhomogeneity of statistical distribution of empirical pairs (χ, δ) on χ–δ plane. Figure 8 shows clearly that the cluster of empirical (χ, δ) is stretched along a line $\chi \sim 1/\delta$ so that estimates of the slopes Φ_1 and Φ should be biased toward a value of -1.

In accordance with the definition of parameters χ and δ, one may suggest several reasons for the cluster of empirical (χ, δ) to be stretched along the slope −1.

First, because $\chi \sim f/N$ and $\delta \sim N/f$, parameters χ and δ are not independent, and any variation in N whether it is caused by "instrumental" noise (i.e., measurement errors), or "physical" noise (e.g., changes of N due to internal waves), or truly related to intrusion dynamics, will stretch the cluster of empirical (χ, δ) toward the slope −1. However, we exclude this possibility because only the pairs with nearly constant value of N have been chosen for the analysis.

Second, since $\delta \sim \gamma_\rho$ and $\chi \sim 1/\gamma_S$, internal waves would simultaneously add the same value of a random "physical" noise to both γ_ρ and γ_S, stretching the cluster of empirical (χ, δ) toward the slope −1. Moreover, the same effect could be produced by coherent variations of γ_ρ and γ_S in frontal meanders and mesoscale eddies. The last variations have a timescale larger than that of intrusion growth and may not be considered as a noise.

Unfortunately, we have no idea whether one can separate stretching of empirical (χ, δ) toward the slope −1 due to the noise from the "true" stretching related to intrusion dynamics, and we cannot estimate the value of bias in Φ_1 and σ. However, in Figs. 7 and 8, we can see a tendency that at $\lg\chi > 1$ the slope of bottom boundary of low σ_T region, Φ_1, becomes considerably less than −1 despite the possibility of bias toward a value of −1. Moreover, Figs. 7 and 8 do display clearly the minimum of σ_T at $\chi\delta \approx 1$ and larger values of σ_T both at $\chi\delta \gg 1$, $\delta \ll 1$ and $\chi\delta \ll 1$, $\delta \ll 1$ which is qualitatively in accordance with numerical calculations shown in Fig. 3, and does not fit those of Fig. 5. Therefore, we may suggest that in the case of data from the Azores Front the power of Ri dependence of turbulent mixing coefficient (21), σ, is less than 1.

6. Conclusions

In this paper, we have examined the effects of double diffusion and turbulent mixing on interleaving in baroclinic ocean fronts in the framework of linear stability approach. We focused on receiving the proper criteria for instability and the dependencies of maximum growth rate of growing intrusions upon the geostrophic Richardson number. An important result of this study is the conclusion that the viscous/diffusive destabilization of geostrophic flow is possible at any (large) value of Ri provided that the momentum/mass transfer is governed by double diffusion. This differs essentially from the case of nondouble-diffusive interleaving in the baroclinic front which cannot occur unless $\mathrm{Ri} < (\mathrm{Pr} + 1)^2/4\ \mathrm{Pr}$ (McIntyre 1970).

In the thermohaline, baroclinic front, double-diffusive interleaving can be controlled by the thermohaline factors (i.e., the horizontal gradient of salinity), baroclinic factors (i.e., the horizontal gradient of density), and both, depending on the value of $\chi\,\mathrm{Ri}^{-1/2}$ (Kuzmina and Rodionov 1992). At $\chi\,\mathrm{Ri}^{-1/2} \ll 1$, interleaving is controlled by the thermohaline factors, and the baroclinicity does not affect interleaving. At $\chi\,\mathrm{Ri}^{-1/2} \gg 1$, interleaving is controlled by the baroclinic factors, and the maximum growth rate of intrusions $\omega'_{\max}$ can be much greater than that of the case $\chi\,\mathrm{Ri}^{-1/2} \ll 1$. If isohaline and isopycnal slopes have the same sign (provided that the stratification is favorable for salt fingering), $\omega'_{\max}$ will increase monotonically with the geostrophic Froude number $\delta \equiv \mathrm{Ri}^{-1/2}$. In the case of opposing isohaline and isopycnal slopes, the terms describing effects of thermohaline and baroclinic factors on instability have opposite signs, that is, work against each other, and $\omega'_{\max}$ vanishes at $\chi\delta = 1$; this case was considered in detail by May and Kelley (1997).

The situation is complicated largely if one takes into account turbulent mixing. In general, turbulent mixing works to suppress the double-diffusive interleaving, whether it be controlled by the thermohaline or baroclinic factors. Namely, if we "switch on" turbulent mixing, $\omega'_{\max}$ will decrease no matter what magnitudes of the input parameters were chosen.

If the coefficient of turbulent mixing, k^*, is independent of Ri, we will get to two types of the δ dependence of $\omega'_{\max}$. At small k^*, $\omega'_{\max}$ is positive in the whole range of δ. When k^* is large enough, there are no positive values of $\omega'_{\max}$ at small $\delta \ll 1$.

In the case of Ri-dependent coefficient of turbulent mixing, it is possible that positive values of $\omega'_{\max}$ do not occur in some intermediate range of $\delta \in [a,\ b]$, $a < b < 1$, where a and b are some functions of the input parameters.

We have formulated several asymptotic criteria that govern the behavior of $\omega'_{\max}(\delta)$ under the effect of turbulent mixing. These criteria were successfully applied to explain the results of numerical calculations of $\omega'_{\max}(\delta)$.

Finally, we have applied the above theory to the ocean intrusions, namely the finestructure intrusions in the Azores front/current. Analyzing empirical estimates of intensity of the intrusions, σ_T, we found a promising resemblance in the behavior of empirical $\sigma_T(\chi,\ \delta)$ and theoretical $\omega'_{\max}(\chi,\ \delta)$. This convinced us that the above theory can be used to describe features of interleaving in the ocean.

Acknowledgments

This research was made possible in part by Grant 97-05-65381 from the Russian Foundation for Basic Research. We are grateful to anonymous reviewers for valuable remarks.

REFERENCES

Fedorov, K. N., 1986: *The Physical Nature and Structure of Oceanic Fronts.* Springer-Verlag, 333 pp.

Korn, G. A., and T. M. Korn, 1968: *Mathematical Handbook for Scientists and Engineers: Definitions, Theorems and Formulas for Reference and Review.* McGraw-Hill, 1130 pp.

Kunze, E., 1994: A proposed flux constraint for salt fingers in shear. *J. Mar. Res.,* **52,** 999–1016.

Kuzmina, N. P., 1997: Intrusions in frontal zones with high thermoclinicity and baroclinicity. *Dokl. Acad. Sci.,* **354,** 114–116.

— ,1998: Mechanisms of water intrusion layering in the Azores frontal zone. *Izv. Acad. Sci. USSR, Atmos. Oceanic Phys.,* **34,** 267–273.

— ,and V. B. Rodionov, 1992: Influence of baroclinicity on the formation of thermohaline intrusions in ocean frontal zones. *Izv. Acad. Sci. USSR, Atmos. Oceanic Phys.,* **28,** 804–810.

May, B. D., and D. E. Kelley, 1997: Effect of baroclinicity on double-diffusive interleaving. *J. Phys. Oceanogr.,* **27,** 1997–2008. Find this article online

McDougall, T. J., 1985a: Double-diffusive interleaving. Part I: Linear stability analysis. *J. Phys. Oceanogr.,* **15,** 1532–1541. Find this article online

— ,1985b: Double-diffusive interleaving. Part II: Finite amplitude, steady state interleaving. *J. Phys. Oceanogr.,* **15,** 1542–1556. Find this article online

McIntyre, M. E., 1970: Diffusive destabilization of the baroclinic circular vortex. *Geophys. Fluid Dyn.,* **1,** 19–57.

Niino, H., 1986: A linear stability theory of double-diffusive horizontal intrusions in a temperature-salinity front. *J. Fluid Mech.,* **171,** 71–100.

Ruddick, B., and J. S. Turner, 1979: The vertical length scale of double-diffusive intrusions. *Deep-Sea Res.,* **26A,** 903–913.

Stern, M. E., 1967: Lateral mixing of water masses. *Deep-Sea Res.,* **14,** 747–753.

Stommel, H., and K. N. Fedorov, 1967: Small-scale structure in temperature and salinity near Timor and Mindanao. *Tellus,* **19,** 88–97.

Toole, J., and D. T. Georgi, 1981: On the dynamics and effects of double-diffusively driven intrusions. *Progress in Oceanography,* Vol. 10, Pergamon, 123–145.

Turner, J. S., 1973: *Buoyancy Effects in Fluids.* Cambridge University Press, 368 pp.

Walsh, D., and B. Ruddick, 1995: Double-diffusive interleaving: The influence of nonconstant diffusivities. *J. Phys. Oceanogr.,* **25,** 348–358. Find this article online

Zhurbas, V. M., N. P. Kuzmina, and I. D. Lozovatskiy, 1988: The role of baroclinicity in intrusive layering in the ocean. *Oceanology,* **28,** 34–36.

— ,— ,R. V. Ozmidov, N. N. Golenko, and V. T. Paka, 1993: Manifestation of subduction in thermohaline fields of vertical finestructure and horizontal mesostructure in the Azores Front/Current. *Oceanology,* **33,** 277–281.

APPENDIX

7. List of Notations

A	The coefficient in the Ri dependence of ζ; see (21)
A_1, A_2	Some critical values of A
C_0, C_1, C_2, C_3	Coefficients of the growth rate polynomial (10)
f	The Coriolis parameter
g	The gravitational acceleration
$H = (\mathrm{Pr}k/f)^{1/2}$	The vertical scale of intrusion
k, k^*	Apparent diffusivities due to salt fingering and turbulence, respectively
L	A horizontal scale of intrusion
l, m	Cross-front and vertical wavenumbers, respectively
$l' = lL$, $m' = mH$	Nondimensional wavenumbers

N	The Brunt–Väisälä frequency
n	The salt fingering flux ratio
$p, \overline{p}$	The perturbation and mean pressure, divided by ρ_0, respectively
Pr	The Prandtl number
Q_0, Q_1, Q_2, Q_3	Coefficients of the nondimensional growth rate polynomial (10′)
$\mathrm{Ri} = (f/N\gamma_\rho)^2$	The geostrophic Richardson number
$\mathrm{Ri}_1^*, \mathrm{Ri}_2^*, \mathrm{Ri}_3^*, \mathrm{Ri}_M^*$	Some critical values of Ri
$R_\rho = \alpha\overline{T}_z/\beta\overline{S}_z$	The density ratio for salt fingering
$S, \overline{S}$	The perturbation and mean salinity, multiplied by β
$T, \overline{T}$	The perturbation and mean temperature, multiplied by α
u, v, w	Cross-front, along-front, and vertical perturbations of velocity, respectively
$\overline{v}$	The along-front mean velocity;
x, y, z	Cross-front, along-front, and vertical coordinates, respectively
α, β	The thermal expansion and salinity contraction coefficients, respectively
$\gamma, \gamma_\rho, \gamma_S$	Cross-front slopes of the intrusion, and density and salinity isolines, respectively
$\delta \equiv \mathrm{Ri}^{-1/2}$	The geostrophic Froude number (parameter of baroclinicity)
$\delta_1, \delta_2, \delta_3$	Some critical values of δ
$\varepsilon_z = (1 - n)/(R_\rho - 1)$	A nondimensional parameter introduced by Toole and Georgi (1981)
$\zeta = k^*/k$	The ratio of turbulent to salt fingering vertical diffusivities
$\rho, \overline{\rho}$	Perturbation and mean density, divided by the reference density ρ_0, respectively
σ	The power in the Ri-dependence of ζ; see (21)
$\chi = f/N\varepsilon_z\lvert\gamma_S\rvert$	A nondimensional parameter introduced by Kuzmina and Rodionov (1992)
$\omega, \omega' = \omega H^2/k$	Dimensional and nondimensional growth rates, respectively

(Click the equation graphic to enlarge/reduce size)

Figures

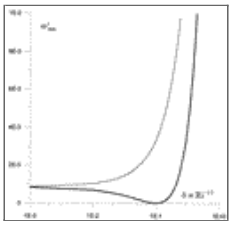

Click on thumbnail for full-sized image.

Fig. 1. The maximum growth rate, $\omega'_{\max}$, vs $\delta \equiv \mathrm{Ri}^{-1/2}$ at Pr = 1, χ = 10, A = 0, $\mathfrak{E}_z$ = 0.5; sgn($\gamma_\rho\gamma_S$) = 1 (top curve) and sgn($\gamma_\rho\gamma_S$) = −1 (bottom curve)

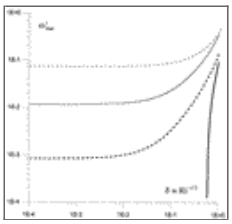

Click on thumbnail for full-sized image.

Fig. 2. The same as in Fig. 1 but for the following input parameters:Pr = 1, $\mathfrak{E}_z$ = 0.5, σ = 0, sgn($\gamma_\rho\gamma_S$) = 1 (all the curves); χ = 10, A = 0.1 (bold solid); χ = 10, A = 0 (bold dashed); χ = 1, A = 0.1 (solid); χ = 1, A = 0 (dashed)

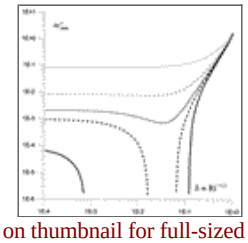

Click on thumbnail for full-sized image.

Fig. 3. The same as in Fig. 1 but for the following input parameters:Pr = 10, $\mathfrak{E}_z$ = 0.5, A = 0.25, σ = 0.5, sgn($\gamma_\rho\gamma_S$) = 1 (all the curves);χ = 100 (bold solid), 30 (bold dashed), 20 (solid), 10 (dashed), 3 (dotted)

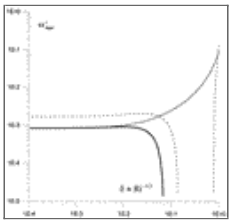

Click on thumbnail for full-sized image.

Fig. 4. The same as in Fig. 1 but for the following input parameters:σ = 1, χ = 10, $\mathfrak{E}_z$ = 0.5, sgn($\gamma_\rho\gamma_S$) = 1 (all the curves); Pr = 1, A = 1 (bold solid); Pr = 1, A = 0.1 (solid); Pr = 2, A = 1 (dashed)

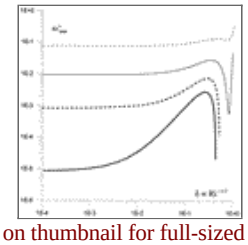

Click on thumbnail for full-sized image.

Fig. 5. The same as in Fig. 1 but for the following input parameters:A = 1, σ = 2, Pr = 1, $\mathfrak{E}_z$ = 0.5, sgn($\gamma_\rho\gamma_S$) = 1 (all the curves), and χ = 100 (bold solid), 10 (bold dashed), 3 (solid), 1 (dashed)

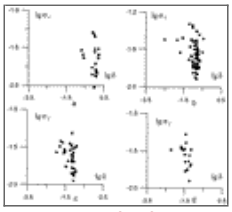

Click on thumbnail for full-sized image.

Fig. 6. Empirical dependencies of the intensity of intrusions σ_T upon the baroclinicity parameter $\delta \equiv \mathrm{Ri}^{-1/2}$ in the Azores Front. The dependencies are drawn up only for a branch controlled by thermohaline factors ($\chi\delta < 2$), and for the following ranges of χ: (a) $1 \leqslant \chi < 2$, (b) $5 \leqslant \chi < 10$, (c) $15 \leqslant \chi < 20$, and (d) $25 \leqslant \chi < 30$

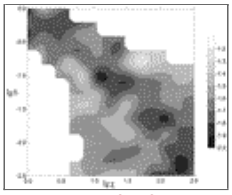

Click on thumbnail for full-sized image.

Fig. 7. A map of intensity of intrusions lgσ_T vs lgχ and lgδ in the Azores Front. Gaps in the map show that the respective values of (χ, δ) are not observed in this particular front

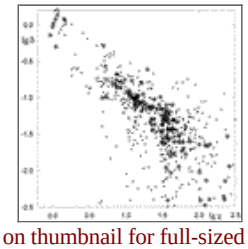

Click on thumbnail for full-sized image.

Fig. 8. A cluster of empirical pairs (χ, δ) used in the analysis (dots). Dots placed inside circles are pairs (χ, δ) with low values of the intrusion intensity lg$\sigma_T < -1.8$

Corresponding author address: Dr. Natalia Kuzmina, Shirshov Institute of Oceanology, Nakhimovsky Prospect 36, 117851 Moscow, Russia.
E-mail: zhurbas@aha.ru

top